# ANALYSING TOPO-GEODETIC, GPR AND INSAR METHOD INTEGRATION FOR HYDROPOWER DAM DEFORMATION MONITORING: CASE STUDY ON THE POIANA MĂRULUI DAM, ROMANIA

**Alexandra G. GEREA**[1,2,3], **Andrei E. MIHAI**[1]

[1]*National Institute for Earth Physics Romania (INCDFP), 12 Călugăreni St., 077125, Măgurele, Ilfov, România*
[2]*University of Bucharest, Doctoral School of Geology, 1 Nicolae Bălcescu Blvd., 01004, Bucharest, Romania*
[3]*University of Birmingham, School of Engineering, Y8, Edgbaston, Birmingham, B15 2FG, United Kingdom*
*e-mail: science.alexandra@gmail.com*

DOI: 10.5281/zenodo.14228987

---

**Abstract.** In Romania, dams undergo extensive evaluations and rigorous surveillance on an annual basis to assess their structural integrity and safety. Conventional monitoring practices primarily involve topo-geodetic techniques, which are crucial for assessing both vertical and horizontal shifts in these structures. However, the application of geophysical methods, such as Ground Penetrating Radar (GPR), has not yet been standardised in their analysis and monitoring protocols. This study explores the feasibility of the GPR surveys and their integration with data from annual levelling surveys from the Poiana Mărului dam, an embankment dam (rockfill with clay-core) located in Caraș-Severin County. Topo-geodetic data are instrumental in providing insights into surface-level changes. Our findings indicate that the GPR approach can significantly augment the existing monitoring framework. It offers valuable insights into the internal composition of specific dam segments, thereby enhancing our understanding of observed phenomena, such as displacements and deterioration, initially identified through topo-geodetic methods. Advanced Differential Interferometric SAR (A-DInSAR) processed data, publicly available from the European Ground Motion Service (EGMS) as a key component of the Copernicus Land Monitoring Service, are considered as well for assessing their suitability in highlighting relevant information about dam deformation monitoring, therefore complementing the ground penetrating radar and topo-geodetical surveys. All of the three methods seem to be correlated in overall general trend in terms of displacements throughout the dam's body, offering insights and information from different perspectives and complementing for providing a much clearer overview of the behaviour of the vertical displacements in time of the dam.

**Key words:** Ground Penetrating Radar, GPR, Levelling, Dams, Hydropower, Monitoring, Topo-geodetic, InSAR, Copernicus

---

## 1. INTRODUCTION

Hydropower dams are critical infrastructure assets, integral to energy generation, water resource management, and flood control. Their longevity and functionality are crucial, yet these structures are subject to ageing (Sims *et al.*, 1994) and deterioration due to natural geological movements and environmental conditions (Prișcu, 1974; Ohmachi *et al.*, 2011). The Poiana Mărului dam in Caraș-Severin County, Romania, an embankment rockfill dam with a clay core, exemplifies these challenges. Embankment dams like Poiana Mărului demonstrate inherent flexibility, but they also experience deformation and displacement over time, attributed to the settling of their constitutive materials, mainly rocks and clays (Popovici, 2002; Cetin *et al.*, 2000).

In Romania, the standard practice for monitoring hydropower dams involves annual or bi-annual topo-geodetical surveys, as mandated by law to ensure optimal operation, maintenance, and accident prevention (Romanian Law nr. 466, 2001). While effective, these traditional surveys may not provide a complete picture of the complex dynamics of dam deformation and displacement. This limitation necessitates the exploration of supplementary monitoring methods (Adamo *et al.*, 2001; Chun Hun, *et al.*, 2018).

This paper introduces a comprehensive approach to dam monitoring by integrating topo-geodetical data with geophysical techniques and satellite-based InSAR technology. More specifically, it focuses on the incorporation of levelling data for monitoring annual vertical displacements at fixed points on the dam (Prişcu, 1974), complemented by the application of Ground Penetrating Radar (GPR). GPR is investigated for its potential to identify areas of interest related to degradation or internal deformation within the dam's crest, thereby providing context and explanations for trends observed in topo-geodetical data (Adamo *et al.*, 2021). Moreover, the paper assesses the application of publicly available processed InSAR data from the European Ground Motion Service (EGMS), a key component of the Copernicus Land Monitoring Service. This assessment aims to evaluate the suitability of InSAR data for monitoring vertical displacements at the Poiana Mărului dam, with a view to establishing a foundation for future, more extensive InSAR data projects. By synthesising these diverse methodologies, the study endeavours to form a holistic monitoring framework for the Poiana Mărului dam, reflecting the concept of assembling a complex puzzle where each component contributes to the dam's safety and efficient operation. This integrative approach not only augments our understanding of the structural behaviour of the Poiana Mărului dam but also proposes a versatile model for enhanced dam monitoring applicable to similar infrastructures both in Romania but also globally.

## 2. MATERIALS AND METHODS

### 2.1. Location

The Poiana Mărului Dam, a rockfill with a clay core embankment dam, is situated on the Bistra Mărului River, in the Caraș-Severin County (Hidroelectrica, 2023), Romania (Fig. 1) and it was commissioned in 1992. Spanning 408 m in length, the dam boasts a narrow crest width of 10 m and rises to a height of 130 m. The reservoir captures water from a 204 km$^2$ basin and integrates additional flows from adjacent basins through secondary intakes, resulting in a substantial accumulation of 96.2 million m$^3$. Geologically, the dam's location is notable for its rocky metamorphic terrain, providing stability to the structure (Hidroconstrucția, 2023). The surrounding slopes, with an average inclination of about 38º, are covered with a relatively thin layer of diluvium. The site was specifically chosen for its confined area, bordered by the bend of the river and the valley's topography. The dam itself features a unique design incorporating anchorages with a clay core, a decision driven by economic and practical considerations.

**Fig. 1.** The location of the Poiana Mărului hydropower dam.

Standing at approximately 130 m, the dam rests on hard, fissured rocky substrates overlaid by deposits around 6-8 m thick (Hidroconstrucția, 2023). More specifically the constituent material is represented by gneisses sourced from a quarry only 4 km away and the clay from about 12 km near the Zăvoi commune. The dam includes a sophisticated water discharge system, consisting of an underground culvert, a cylindrical tower, an underground gallery, and a rapid channel. Additionally, the bottom emptying mechanism, with a pressure intake gallery and flat valves, plays a vital role in managing water flow. For sealing, the dam utilises injection veils and drainage boreholes, integrated into a perimeter gallery below the clay core. Adjacent to the dam, the MHC Poiana Mărului hydropower facility is equipped with a Francis-type turbine and has a unique unclogging mechanism for the turbine flow (Hidroconstrucția, 2023).

### 2.2. Levelling Method

The topo-geodetic method used in this study represents the geometric levelling method. Precision geometric levelling is typically employed to ascertain building subsidence. This involves levelling marks (bench marks) embedded in the structure, aligning them with fixed external reference points forming a supporting network, or the levelling network. This can vary in structure, often comprising closed polygons or parallel traverses, depending on the object's size and shape. It includes marks on the observed structure and external control marks, with their design influenced by local conditions and the construction's material (Fig. 2).

At the Poiana Mărului dam, the levelling network is formed of 8 fundamental (fixed) marks, among which two are placed near the dam keeper's house, and 2 others are placed on each individual berm; and 48 bench marks, placed on the downstream side of the dam and on the crest (Fig. 2). Throughout the years, due to usually environmental, natural and placement of the fixed points, these might suffer movement or even damage themselves, which would make them unsuitable for surveying, therefore reducing the consistency in number of readings occurring every year, and lowering the amount of information to be correlated in some specific areas.

Therefore, the geometric levelling network (Coşarcă, 2003) is established through levelling landmarks, where measurements between these landmarks are taken to determine level differences and route lengths under observation. For effective network adjustment, several elements are essential: measuring level differences using the geometric levelling method; understanding path lengths for determining measurement weights (1), and finally, knowing the altitude of height marks (*Hi*) in the levelling point network. The process involves determining absolute altitudes of new network points, the most likely level differences on measured routes, and the accuracy of these values (Avram *et al.*, 2017).

**Fig. 2.** Overview of the Levelling Network, with visible bench marks on different berms. The position of the GPR profiles on the dam's crest is also shown.

The methodological framework can be either a functional model (Gauss-Markov), focusing on size relationships without random elements (2) where *v* represents the correction vector of the recorded value, *A* represents a coefficients matrix, *x* is a parameter vector and *l* the free terms vector; or a statistical (stochastic) model (3), considering random variables indicating potential displacements and deformations where $\sigma_0^2$ is the unit variance *Qxx=N-1* represents a block extracted from the cofactors matrix (Avram *et al.*, 2017).

$$P_{ij} = \frac{1}{L_{ij[km]}} \tag{1}$$

$$v = Ax - l \tag{2}$$

$$\sum\nolimits_{ll} = \sigma_0^2 Q_{ll} \tag{3}$$

Geometric corrections (Coșarcă, 2003) are determined for compensated values of unknown size (4) and differences in measured levels (5), followed by normalisation and solving of the system of linear correction equations. This procedure yields corrections for new point altitudes (6) and level differences (7), where *N* represents the normal matrix of the system of equations, *A* is the system of equations which describes the matrix correction coefficients, *P* represents the weight matrix, *x* is the vector of unknown elements and finally *l* is the matrix describing the free terms (Avram, *et al.*, 2017). The accuracy elements involve calculating the standard deviation of unit weight (8) - where n represents the total number of measured level differences and h is the number of unknown points in the network; the standard deviation of individual level differences (9), and of the indirectly determined quantities (10), contributing to the overall accuracy of altitude determinations in the network (11).

$$H_i = H_i^0 + x_1 \text{, where } i = 1,2,\dots,n \tag{4}$$

$$\Delta h_{ij} = H_{ij}^0 + v_{ij} \tag{5}$$

$$N = A^T PA \tag{6}$$

$$x = -N^{-1} A^T Pl \tag{7}$$

$$S_0 = \sqrt{\frac{[pvv]}{n-h}} \tag{8}$$

$$S_i = \frac{S_0}{\sqrt{P_i}} \text{, where } i = 1,2,\dots,n \tag{9}$$

$$\left(S_x\right) = S_0 \cdot \sqrt{q_{jj}} \text{, where } i = 1,2,\dots,n \tag{10}$$

$$S_t = \frac{1}{h}\sum_{j=1}^{h}\left(S_x\right)_j \tag{11}$$

Surveys were carried out using the high precision equipment, Leica Sprinter with 3 m levelling barcode staffs, and a 5 kg levelling staff base, to carry out the measurements for the detection of vertical displacements, in the 2016 and 2017 data, as described by Stănescu *et al.*, 2017. However, for this paper, data from 2008-2013 are also considered for a better overview of the vertical displacements in the dam, where the equipment used must comply with the same precision standard due to the national regulations and laws for dam monitoring in Romania (STAS 2745/90).

More specifically, the chosen levelling method was the middle geometric levelling of the first order (Nistor, 1993). For the data processing the compensation chosen for the levelling network, was the conditioned compensation of the measurements with different precisions (Nistor, 1998).

### 2.3. Ground Penetrating Radar Method

The Ground Penetrating Radar (GPR) method represents a complex geophysical technique for subsurface imaging, utilising electromagnetic waves to detect and characterise various subsurface objects and anomalies. This non-invasive approach is extensively employed in a variety of studies ranging from archaeological, to geotechnical, geological studies, with the method even being recently applied to studies of geological mapping on Mars, with significant potential and outcomes (Hamran *et al.*, 2022). In geotechnical studies the GPR method is widely used for monitoring deformations and damages in road pavements, bridges stability studies, railway gravel inspection, damage caused by cracks in concrete inspection studies (Batrakov *et al.*, 2017), mapping water infiltrations and sinkholes (De Giorgio *et al.* 2014). In the past few years, more research has emerged in terms of possibilities of using the method on hydropower dams, which represent sensitive subjects in their nature due to their economic impact and devastating outcomes if these structures are prone to damage and failing due to their degradation in time.

The typical GPR equipment comprises a control console, responsible for setting acquisition parameters and managing the antenna operations, including automatic measurements. Additionally, it features a distance-measuring wheel for profiling georadar distances and an antenna operating at frequencies usually ranging from 150 MHz to 8 GHz, tasked with emitting and receiving electromagnetic signals (Daniels, 2004).

The fundamental operating principle of GPR involves the transmission of electromagnetic waves into the subsurface by the antenna. These waves travel through the medium at a velocity determined by the material's permittivity *ε* (or dielectric constant). While moving the antenna over the ground, the antenna emits electromagnetic pulses, which upon encountering materials or objects with different permittivity values, the signal partially reflects back to the surface antenna where it is recorded, while another portion of the energy continues to travel through the environment until it is eventually attenuated (Reynolds, 2011). During this process, the antenna continuously transmits signals at a pre-set frequency, determined via the console, with data recording occurring within a pre-selected time window (Conyers, 2004). GPR data is captured in a similar format to seismic methods, represented as vertical traces over time. The cumulative adjacent traces, resulting from the antenna's movement across the surveyed surface, forms a two-dimensional image known as a radargram, displaying distance along the x-axis and time along the z-axis (Conyers, 2004). Reflections within the radargram typically manifest as hyperbolas due to the antenna's ovaloid footprint and its varying interception angles of the same object during movement. The transformation of data from the time domain to the spatial domain, known as migration, involves mathematical transforms that align the hyperbolic reflections with the actual dimensions and shapes of the subsurface objects (Reynolds, 2011).

The selection of a specific antenna frequency is contingent upon the study's objectives. A general rule is that higher frequencies yield more detailed information but at shallower depths, whereas lower frequencies facilitate deeper penetration but with reduced detail.

In dam monitoring GPR has the capability to provide a characterization of the internal structure (Pueyo Anchuela, 2018) with the help of radargrams allowing for an in depth analysis of internal features (Loperte *et al.*, 2011), like foundations level (Gerea, 2023), water inclusions or seepage (Kayode, 2018), subsidence levels, voids (Xu *et al.*, 2010), degradation areas, and so on. By visualising these elements and conducting repeated measurements over time, GPR effectively contributes to understanding and monitoring the stability and temporal evolution of structural integrity in such constructions.

At the Poiana Mărului dam, the surveys were carried out using a GSSI SIR-3000 GPR equipment consisting of a console, a wheel and a 200 MHz antenna (Fig. 3). The device is not specialised for geotechnical measurements and does not present standardised functions for identifying construction elements, this being a complex and flexible equipment that can be used in all fields of interest as long as the antenna used is the right one for the studied objective, and the parameters procurement are carefully selected to highlight the objectives. Data was collected in the form of two parallel profiles (Fig. 2) positioned on the crest of the dam, on its cubic stone surface (Fig. 4), approximately 4 m away from the dam's crest safety fences. For analysing the first top layers of the dam's crest and to make sure that no interferences from the side walls would add more unwanted noise to the radargrams and influence the data quality.

**Fig. 3.** The GSSI SIR-3000 GPR system used to collect the GPR data, consisting of a 200 MHz antenna, a wheel and a console.

**Fig. 4.** Overview on the dam's crest, highlighting the pavement conditions visible at the surface.

The data was processed using ReflexW, a GPR and seismic processing software, and both radargrams followed the same steps and the same filter parameters, following a sequence of signal processing steps which start with geometrical correction, followed by the application of 1D filters, which act on individual traces, and 2D filters which act on more traces at a time, and finishing steps to amplify the signals of interest and transforming from time domain to distance domain through migration. Several processing methodologies and sequences of filter applications have been tested and analysed, but this sequence of functions and filters succeeds in highlighting features of interest within the dam crest without overly distorting the underlying information.

The specific data processing functions and their order is as follows:

(i) Trace exclusion was performed using the 'remove range' function to eliminate the initial section of data, specifically for the Poiana Mărului dam radargrams.

(ii) The zero time adjustment was achieved through the 'move startime' function.

(iii) Low-frequency noise was mitigated using the 'subtract-mean' (dewow) function.

(iv) Frequencies outside the antenna's operational range were filtered out employing a 'butterworth bandpass filter,' targeting both low and high-frequency ranges.

(v) Systematic coherent noise, known as ringing, was reduced by applying the 'background removal' function, which involves subtracting an average trace.

(vi) Signal amplification was conducted using the 'gain' function, focusing on energy decay.

(vii) 'fk-Stolt migration' tool was used by applying a velocity setting of 0.12 m/ns (based on the hyperbola fitting tool), for transforming data from time domain to distance and reducing the appearance of the hyperbolas.

After data processing, several elements that are part of the internal structure of the dam could be identified and delimited.

### 2.4. The InSAR method

Interferometric Synthetic Aperture Radar (InSAR) is a cutting-edge remote sensing technology that has revolutionised the monitoring of Earth's surface changes, which can also be useful in dam deformation monitoring. InSAR utilises the phase differences of radar signals emitted from satellites to detect subtle surface deformations. The technique involves sending radar pulses from space and measuring the time it takes for these pulses to be reflected back to the satellite. The phase of these radar signals – which indicates the position of a wave cycle at a specific moment – is crucial in InSAR analysis. By comparing the phase of the signals at different times, InSAR can detect with up to millimetre level precision changes in the Earth's surface, and is especially effective in vertical deformations or subsidence monitoring analysis (Alonso-Díaz, 2023). This capability is particularly significant in monitoring the structural health of dams, where even small displacements can indicate potential issues (Prișcu, 1974). Unlike traditional ground-based monitoring techniques, InSAR can provide a comprehensive view of surface deformations over the entire area of a structure.

The European Ground Motion Service (EGMS), a component of the Copernicus Land Monitoring Service, provides processed InSAR data, making this technology more accessible for various applications, like analysing sinkholes in urban areas (Busetti *et al.*, 2020), subsidence monitoring in coastal areas (Alonso-Díaz *et al.*, 2023) and including the monitoring of embankment dams (Ruiz-Armenteros *et al.*, 2021), which is attempted in this study. EGMS offers consistent, continent-wide ground motion measurements, leveraging the capabilities of the Copernicus Sentinel-1 satellites. In terms of applications of InSAR on embankment dams have demonstrated its effectiveness in various contexts. For instance, the monitoring of the displacement and potential settlement in large dam structures has been successfully conducted using InSAR data, providing key insights into the behaviour of these dams under different environmental and operational conditions (Marchamalo-Sacristán *et al.*, 2023). Such applications underscore the potential of InSAR, in complementing traditional methods like levelling surveys and ground-penetrating radar, offering a more comprehensive understanding of dam behaviour and enhancing the capability to ensure their safety and longevity.

The application of EGMS InSAR data in monitoring embankment dams like the Poiana Mărului dam represents a significant advancement in ensuring their structural integrity. InSAR data from EGMS allows for the detection of displacement trends at an almost real-time monitoring level (every 6 days based on satellite orbit period of the Sentinel-1 pair of satellites), without any other intervention on the field, this representing being a remote sensing method, even though limited by resolution.

In terms of available data in this paper only the Ortho products have been used, representing the calibrated products derived from ascending and descending paths, and possess distinct acquisition geometries (Capes & Passera, 2021). This results in a non-identical distribution of measurement points (MPs) across the two datasets. To guarantee that both datasets accurately represent the same ground area, the data is averaged onto a shared 100 m grid. This specific grid spacing aligns with other Copernicus services, offering a balanced trade-off between the resolution of the data and the spatial extent covered by the database (Capes & Passera, 2021). Radar backscattering is the process where a target object reflects a part of the radar energy back towards the radar antenna. This occurs when a radar signal emitted by a satellite comes into contact with an object on Earth, causing some of the signal to scatter back towards the source. The radar then captures this backscattered energy. The intensity of this backscattered signal determines the luminosity of each pixel in an image (Detektia, 2024). Consequently, interpreting images from synthetic aperture radar (SAR) can be complex due to this relationship between the backscattered signal and the image brightness. Therefore two types of ground measurement points can be described, the permanent Scatterers or PS, which represent radar targets that exhibit high reflectivity, leading to notably bright pixels in the SAR imagery (Detektia, 2024). Typically, they correspond to discrete man-made structures; and the distributed Scatterers or DS, which are often represented by clusters of adjacent pixels in the SAR image, each displaying a similar radar signature. Despite the presence of temporal decorrelation phenomena, these scatterers still enable the extraction of displacement data. They generally correspond to extensive areas showing uniform phase behaviour (Detektia, 2024).

Therefore in terms of spatial resolution, the PS full resolution, represented by the single pixel of Sentinel-1 constellation products in Interferometric Wide Swath is 5 × 20 m, and for the DS is better than 100 m, and a temporal resolution of 6 days from 2016 onwards (Capes & Passera, 2021). The mean velocity resolution is less than 1 mm/year and the 3D geolocation accuracy is better than 10 m.

For the Poiana Mărului Dam, a number of 17 data set points have been found to overlap with the position and area of the hydropower dam and its surroundings (Fig. 5), among which 15 appear to be covering specifically the dam's body including the crest. Two Orto data sets have been used, a data set ranging from 2018 to 2022, and another data set with fewer points ranging from 2015 to 2021. Data has been downloaded and visualised in ArcGIS Pro, as well as graphs have been analysed on the EGMS platform.

## 3. RESULTS AND DISCUSSION

The levelling data is represented in the form of graphs for each berm including the crest (Figs. 6-10), where the data covers the difference between consecutive years in measured and compensated displacement values for each bench mark. The data starts with 2008 and goes up to 2017, with no data available for the years 2014 and 2015 unfortunately, and due to this, there is a significant variation visible in the graphs which is clearly marked in all graphs at the 2016-2013 data row. Another observation would be given by the fact that data from 2009 even though constant throughout all of the berms in terms of general trending of the data (when comparing with the displacement differences from other year intervals) appears as having much larger values.

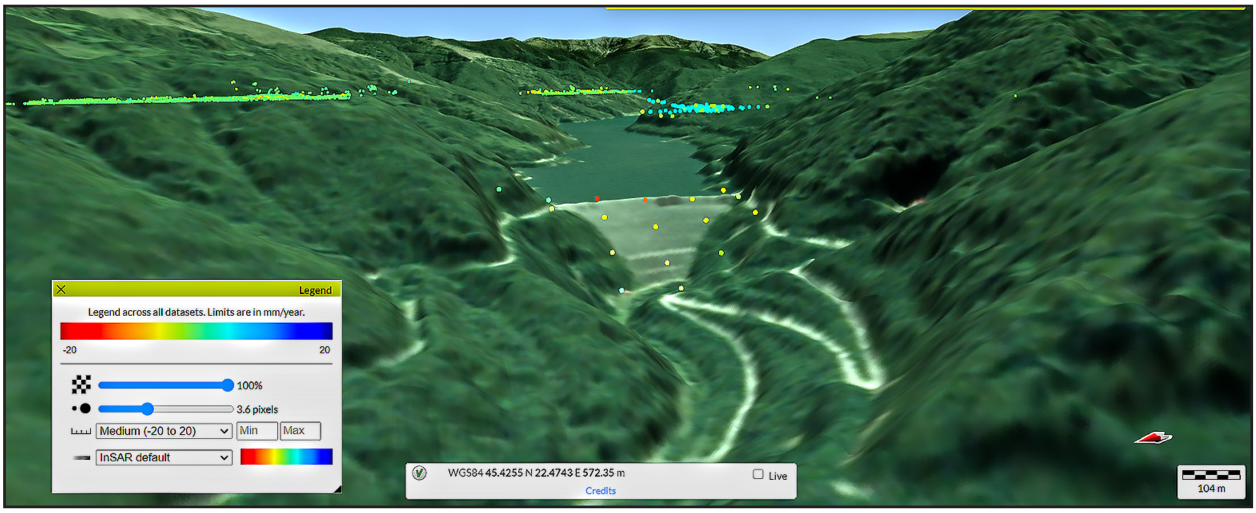
Legend across all datasets. Limits are in mm/year.

**Fig. 5.** 3D overview of the InSAR available data from the EGMS platform for the 2018-2022 data set located at the Poiana Mărului dam.

However, what can be observed in the data, there are some specific trends, especially in the displacement differences in the benchmarks from the crest (Fig. 6). On the crest there appears that on the bench marks numbered 42-44 there appears to be a constant higher gradual displacement from one year to another compared to the benchmarks surrounding these. With a very low displacement variation on the benchmark 48 which is placed closer to the road leading to the dam's crest. A fairly similar pattern, with a larger constant displacement variation, can be observed in the berm just below the crest (Fig. 7), in the 605 m, where it appears as well, a higher variation in the benchmarks 31-33, positioned approximately in the middle area of the dam (similar to the benchmarks from the crest).

Going on the lower berms, in the 585 m berm (Fig. 8) the trend of the benchmarks in terms of displacements, from one side to the other seems to have a similar pattern to the previous two levels, with the middle benchmarks having a higher variety throughout the years. The displacements from the last two berms (Figs. 9-10) seem to have a rather low overall variety throughout the benchmarks compared to the previous ones, and low variety in terms of displacements from one year to another.

The processed GPR data, in the form of radargrams (Fig. 11) appears to highlight certain areas of interest throughout the whole profile, and offer useful reflections or information from up to approximately 4 m below the ground. It appears that the highlighted features appear to be constant on both profiles. The most notable feature is represented by the visibility of 3 top reflective horizons, rather discontinued from one side to the other of the profiles, which can be interpreted as different layers of material, part of the foundation of the road on top of the crest. These horizons appear to change in depth between 140 m - 165 m on the profile's length, marked by a high reflective area at the lowest point of the horizons. This area marks an area of a slight subsidence. On the sides of the profile, there appear to be areas described by stronger reflections, marking a change in material. As the profile was close to the roads on both sides, it is not surprising to see these interferences, which might probably mark the edge of the dam's body. As these represent the first GPR data from the dam's crest, and not being able to compare with previous data from different years, to assess the variation through time, at this stage it can be said that the variation in the depth and width of the horizons represents probably the mixing of the materials in between, as the GPR would normally be able to differentiate between the materials having different permittivity values (sands, clays, etc.). It is not clear what the cause is for this, and if the thickness of the layers has always been inconsistent through the dam's top layers.

In terms of InSAR data, visible in figure 12, the first row of data points shows variation throughout the points of -13.9 mm/year, with higher mean velocities concentrated in the middle, and with decreasing velocities moving outwards (with the highest velocity calculated between 2018-2022). A similar pattern can be observed going down on the next row (Fig. 13), where the most extreme points seem to have lower velocities compared to the points in the interior of the set, with a maximum velocity, for the point in the middle, of -8.4 mm/year. The values appear to be more reduced, when going even further to the next sets (Figs. 14-15), and as moving towards the bottom of the dam (on the downstream side) the variation is also reduce throughout the data sets from one side to the other, but the number of points is reduced as well, from 5 to only 3 and 2 respectively. At the lower levels the maximum velocities appear to be -2.00 mm/year (Fig. 14) and -1.8 mm/year (Fig. 15) in the points with the higher variation. Therefore it can be observed from the area closer to the dam's crest to the bottom of the dam. Apart from the data, what can be observed in the InSAR platform is how isolated in terms of points is the dam's body compared to the surroundings.

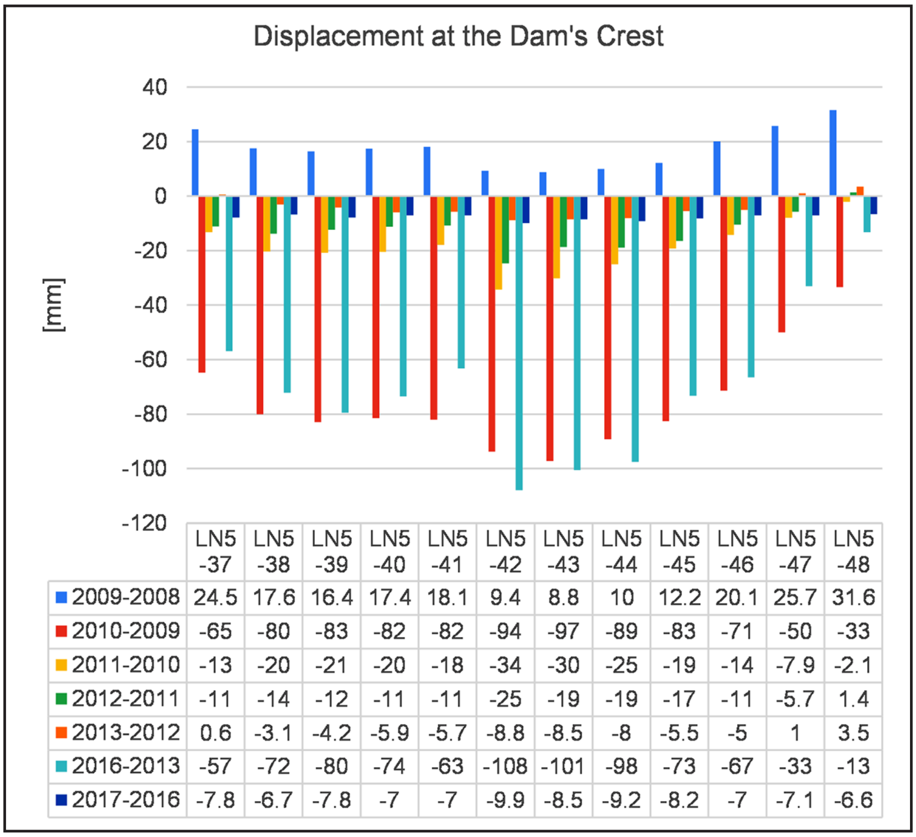

| | LN5 -37 | LN5 -38 | LN5 -39 | LN5 -40 | LN5 -41 | LN5 -42 | LN5 -43 | LN5 -44 | LN5 -45 | LN5 -46 | LN5 -47 | LN5 -48 |
|---|---|---|---|---|---|---|---|---|---|---|---|---|
| ■ 2009-2008 | 24.5 | 17.6 | 16.4 | 17.4 | 18.1 | 9.4 | 8.8 | 10 | 12.2 | 20.1 | 25.7 | 31.6 |
| ■ 2010-2009 | -65 | -80 | -83 | -82 | -82 | -94 | -97 | -89 | -83 | -71 | -50 | -33 |
| ■ 2011-2010 | -13 | -20 | -21 | -20 | -18 | -34 | -30 | -25 | -19 | -14 | -7.9 | -2.1 |
| ■ 2012-2011 | -11 | -14 | -12 | -11 | -11 | -25 | -19 | -19 | -17 | -11 | -5.7 | 1.4 |
| ■ 2013-2012 | 0.6 | -3.1 | -4.2 | -5.9 | -5.7 | -8.8 | -8.5 | -8 | -5.5 | -5 | 1 | 3.5 |
| ■ 2016-2013 | -57 | -72 | -80 | -74 | -63 | -108 | -101 | -98 | -73 | -67 | -33 | -13 |
| ■ 2017-2016 | -7.8 | -6.7 | -7.8 | -7 | -7 | -9.9 | -8.5 | -9.2 | -8.2 | -7 | -7.1 | -6.6 |

**Fig. 6.** Displacement values resulted from the levelling data collected on the dam's crest.

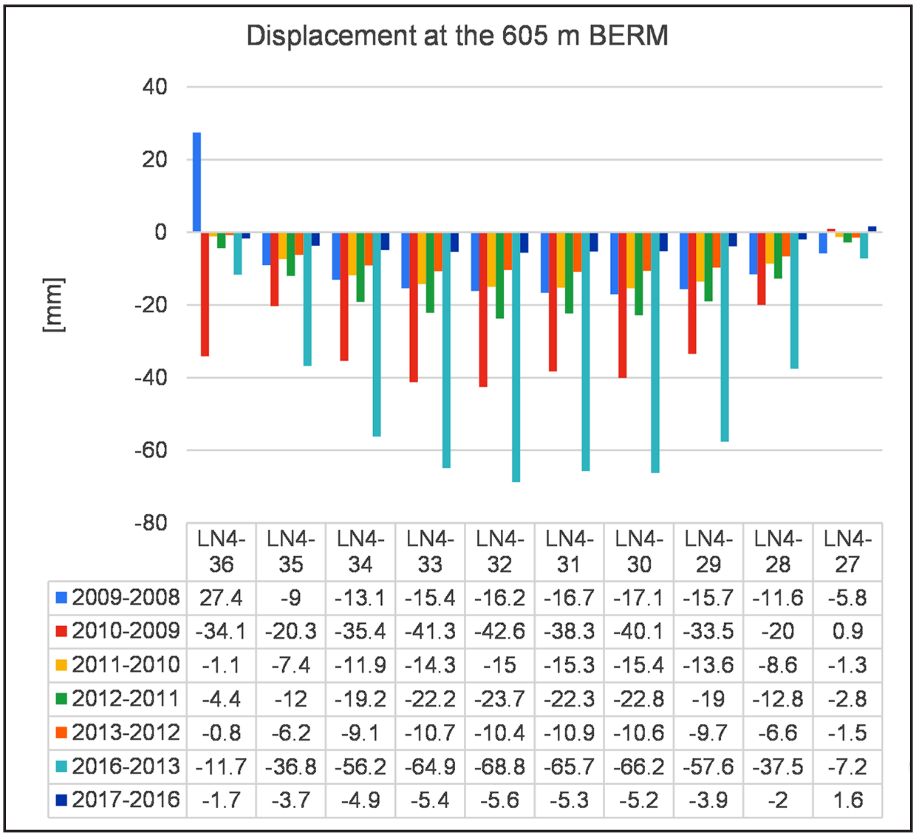

| | LN4-36 | LN4-35 | LN4-34 | LN4-33 | LN4-32 | LN4-31 | LN4-30 | LN4-29 | LN4-28 | LN4-27 |
|---|---|---|---|---|---|---|---|---|---|---|
| ■ 2009-2008 | 27.4 | -9 | -13.1 | -15.4 | -16.2 | -16.7 | -17.1 | -15.7 | -11.6 | -5.8 |
| ■ 2010-2009 | -34.1 | -20.3 | -35.4 | -41.3 | -42.6 | -38.3 | -40.1 | -33.5 | -20 | 0.9 |
| ■ 2011-2010 | -1.1 | -7.4 | -11.9 | -14.3 | -15 | -15.3 | -15.4 | -13.6 | -8.6 | -1.3 |
| ■ 2012-2011 | -4.4 | -12 | -19.2 | -22.2 | -23.7 | -22.3 | -22.8 | -19 | -12.8 | -2.8 |
| ■ 2013-2012 | -0.8 | -6.2 | -9.1 | -10.7 | -10.4 | -10.9 | -10.6 | -9.7 | -6.6 | -1.5 |
| ■ 2016-2013 | -11.7 | -36.8 | -56.2 | -64.9 | -68.8 | -65.7 | -66.2 | -57.6 | -37.5 | -7.2 |
| ■ 2017-2016 | -1.7 | -3.7 | -4.9 | -5.4 | -5.6 | -5.3 | -5.2 | -3.9 | -2 | 1.6 |

**Fig. 7.** Displacement values resulted from the levelling data collected on the 605 m berm.

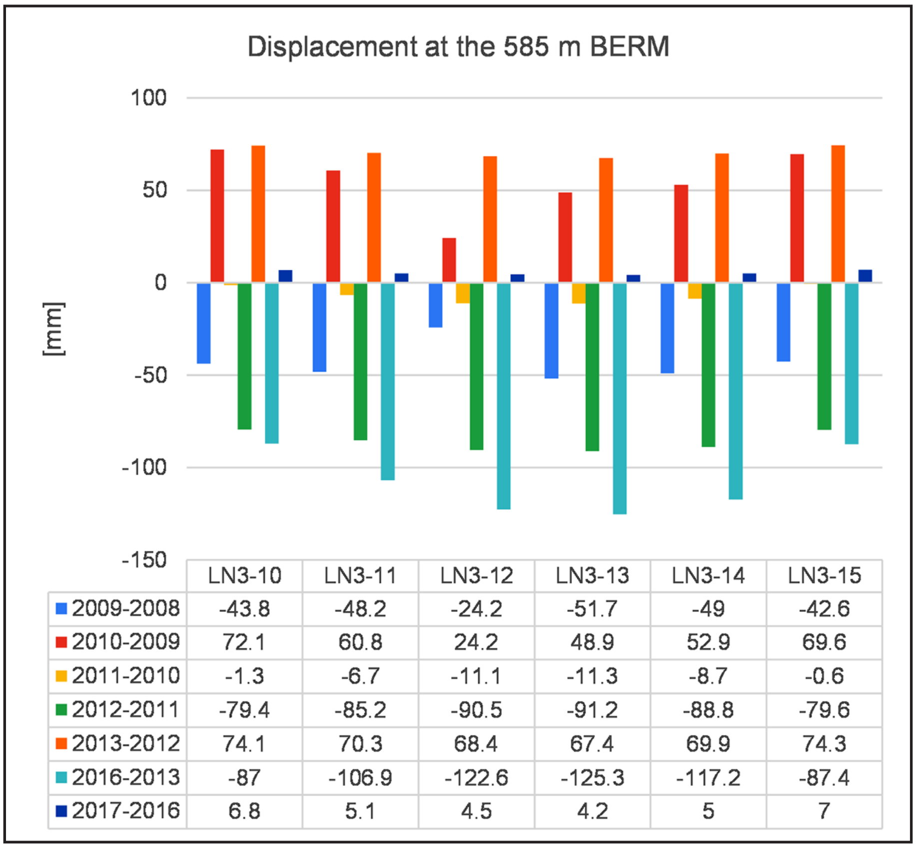

| | LN3-10 | LN3-11 | LN3-12 | LN3-13 | LN3-14 | LN3-15 |
|---|---|---|---|---|---|---|
| 🟦 2009-2008 | -43.8 | -48.2 | -24.2 | -51.7 | -49 | -42.6 |
| 🟥 2010-2009 | 72.1 | 60.8 | 24.2 | 48.9 | 52.9 | 69.6 |
| 🟨 2011-2010 | -1.3 | -6.7 | -11.1 | -11.3 | -8.7 | -0.6 |
| 🟩 2012-2011 | -79.4 | -85.2 | -90.5 | -91.2 | -88.8 | -79.6 |
| 🟧 2013-2012 | 74.1 | 70.3 | 68.4 | 67.4 | 69.9 | 74.3 |
| 🟦 2016-2013 | -87 | -106.9 | -122.6 | -125.3 | -117.2 | -87.4 |
| 🟦 2017-2016 | 6.8 | 5.1 | 4.5 | 4.2 | 5 | 7 |

**Fig. 8.** Displacement values resulted from the levelling data collected on the 585 m berm.

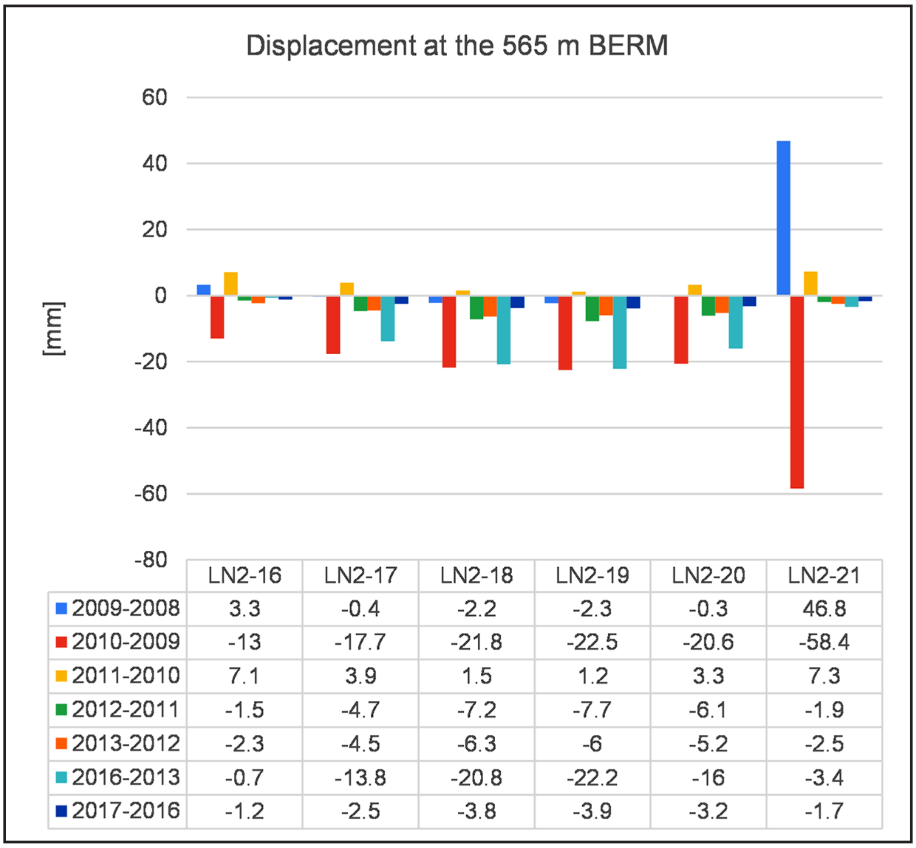

| | LN2-16 | LN2-17 | LN2-18 | LN2-19 | LN2-20 | LN2-21 |
|---|---|---|---|---|---|---|
| 🟦 2009-2008 | 3.3 | -0.4 | -2.2 | -2.3 | -0.3 | 46.8 |
| 🟥 2010-2009 | -13 | -17.7 | -21.8 | -22.5 | -20.6 | -58.4 |
| 🟨 2011-2010 | 7.1 | 3.9 | 1.5 | 1.2 | 3.3 | 7.3 |
| 🟩 2012-2011 | -1.5 | -4.7 | -7.2 | -7.7 | -6.1 | -1.9 |
| 🟧 2013-2012 | -2.3 | -4.5 | -6.3 | -6 | -5.2 | -2.5 |
| 🟦 2016-2013 | -0.7 | -13.8 | -20.8 | -22.2 | -16 | -3.4 |
| 🟦 2017-2016 | -1.2 | -2.5 | -3.8 | -3.9 | -3.2 | -1.7 |

**Fig. 9.** Displacement values resulted from the levelling data collected on the 565 m berm.

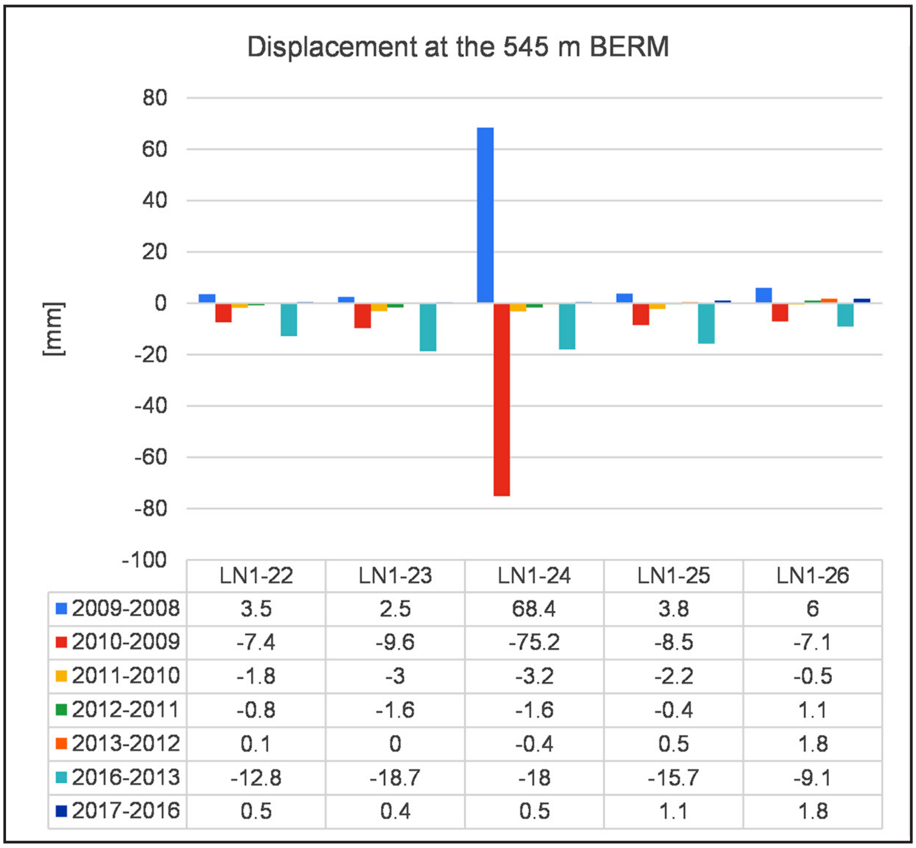

| | LN1-22 | LN1-23 | LN1-24 | LN1-25 | LN1-26 |
|---|---|---|---|---|---|
| ■ 2009-2008 | 3.5 | 2.5 | 68.4 | 3.8 | 6 |
| ■ 2010-2009 | -7.4 | -9.6 | -75.2 | -8.5 | -7.1 |
| ■ 2011-2010 | -1.8 | -3 | -3.2 | -2.2 | -0.5 |
| ■ 2012-2011 | -0.8 | -1.6 | -1.6 | -0.4 | 1.1 |
| ■ 2013-2012 | 0.1 | 0 | -0.4 | 0.5 | 1.8 |
| ■ 2016-2013 | -12.8 | -18.7 | -18 | -15.7 | -9.1 |
| ■ 2017-2016 | 0.5 | 0.4 | 0.5 | 1.1 | 1.8 |

**Fig. 10.** Displacement values resulted from the levelling data collected on the 545 m berm.

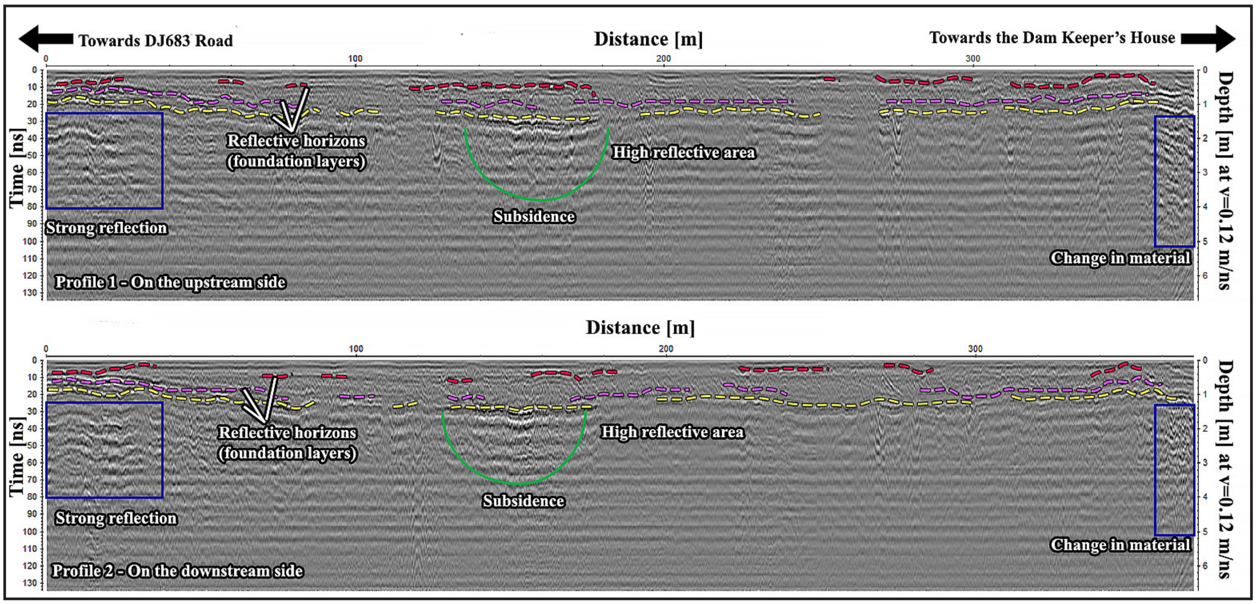

**Fig. 11.** Processed GPR data (radargrams) collected on the dam's crest.

Actually it appears that the Poiana Mărului dam is covered with more data points when compared to larger and more significant hydropower dams from Romania, where in some cases there are none (Gura Apelor, Vidraru, the two largest dams in Romania, for example have low to none InSAR displacement data coverage). This is most probably to the large exposed area

Adding all of the data in ArcGIS and all of the observed information from all of the 3 methods, it appears to be easier to integrate visually the data and extract information with similar behaviours throughout different methods. Therefore, it appears that there exist a couple correlations between different types of data.

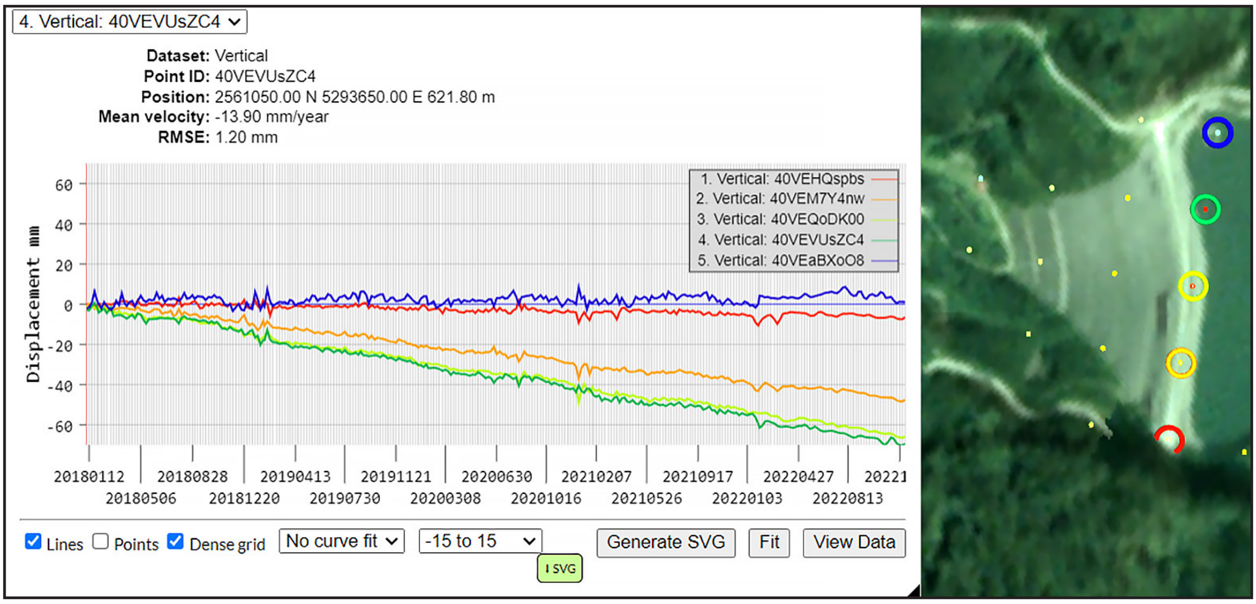
4. Vertical: 40VEVUsZC4

**Dataset:** Vertical
**Point ID:** 40VEVUsZC4
**Position:** 2561050.00 N 5293650.00 E 621.80 m
**Mean velocity:** -13.90 mm/year
**RMSE:** 1.20 mm

☑ Lines ☐ Points ☑ Dense grid
No curve fit
-15 to 15

**Fig. 12.** Vertical displacement values resulted from the InSAR data of the first row of data points.

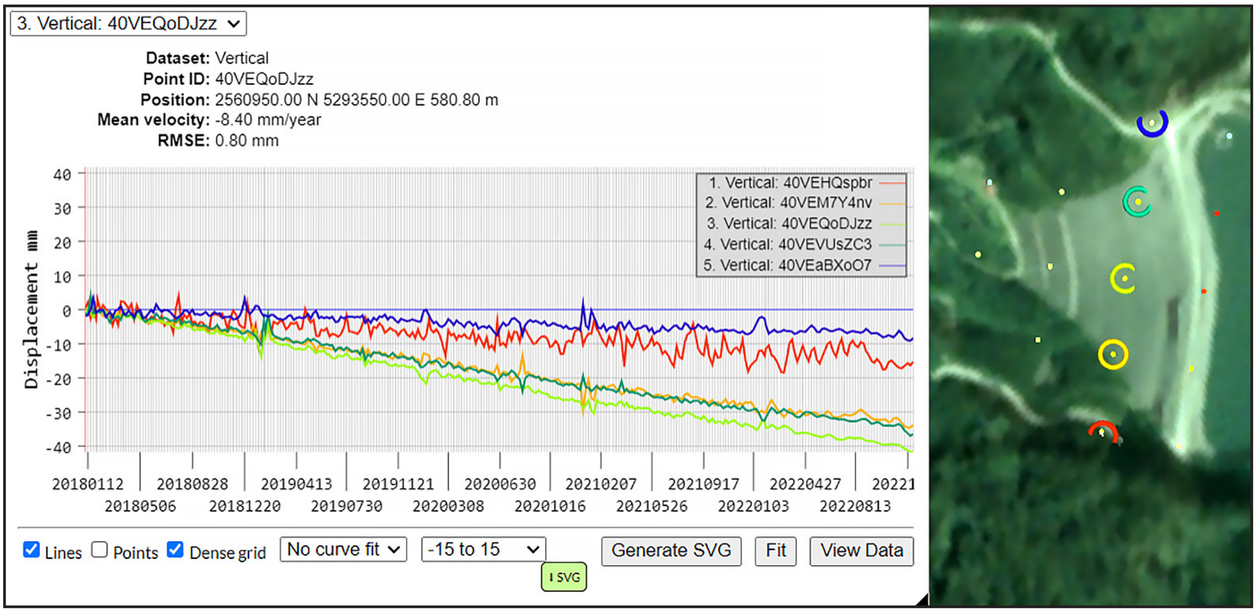
3. Vertical: 40VEQoDJzz

**Dataset:** Vertical
**Point ID:** 40VEQoDJzz
**Position:** 2560950.00 N 5293550.00 E 580.80 m
**Mean velocity:** -8.40 mm/year
**RMSE:** 0.80 mm

☑ Lines ☐ Points ☑ Dense grid
No curve fit
-15 to 15

**Fig. 13.** Vertical displacement values resulted from the InSAR data of the second row of data points.

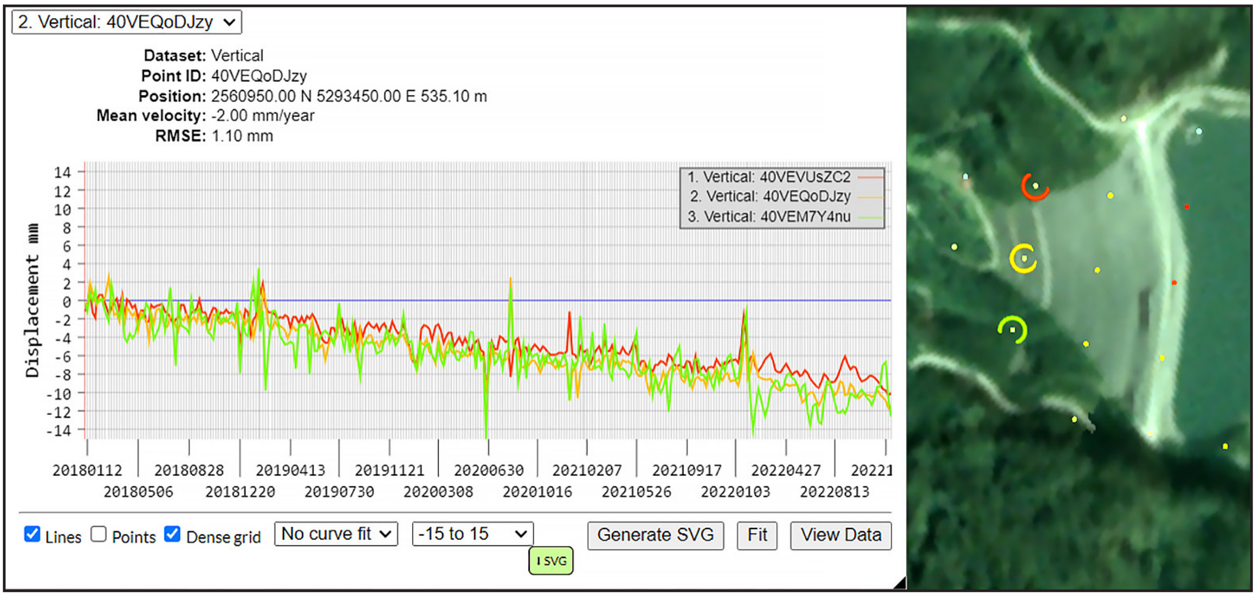

2. Vertical: 40VEQoDJzy

**Dataset:** Vertical
**Point ID:** 40VEQoDJzy
**Position:** 2560950.00 N 5293450.00 E 535.10 m
**Mean velocity:** -2.00 mm/year
**RMSE:** 1.10 mm

☑ Lines ☐ Points ☑ Dense grid No curve fit -15 to 15

**Fig. 14.** Vertical displacement values resulted from the InSAR data of the third of data points.

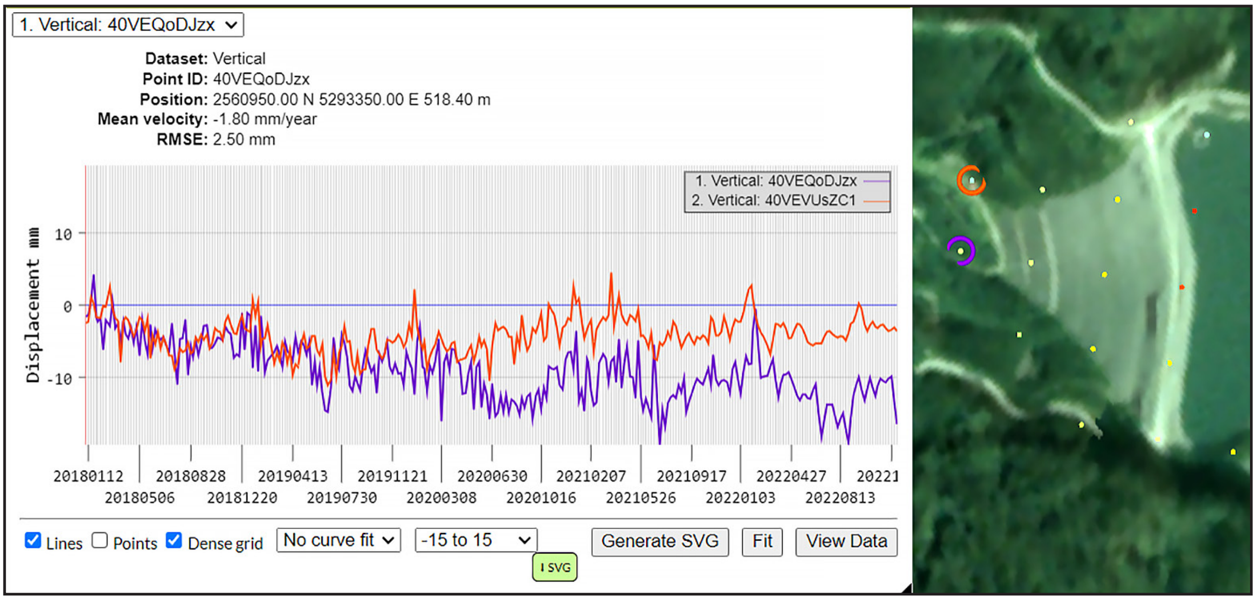

1. Vertical: 40VEQoDJzx

**Dataset:** Vertical
**Point ID:** 40VEQoDJzx
**Position:** 2560950.00 N 5293350.00 E 518.40 m
**Mean velocity:** -1.80 mm/year
**RMSE:** 2.50 mm

☑ Lines ☐ Points ☑ Dense grid No curve fit -15 to 15

**Fig. 15.** Vertical displacement values resulted from the InSAR data of the fourth row of data points.

The data marked in the GPR area as a subsidence (Fig. 11), appears to correlate with the area marked by the 42-44 benchmarks (Fig. 6), whereas the horizons appear to be slightly higher in the extremities of the profiles.

When it comes to the InSAR data, even though the pixel size is quite large, the precision of the pixels is still very good, and different patterns can be observed for example in the InSAR data from the 2018-2022 data set (Fig. 16). Similar to the overall trend of the displacement data resulting from the levelling method (Figs. 6-10), there appears to be a slightly higher negative displacement value right across the middle of the dam from the crest of the dam to the lowest berm. The points of highest variation from each berm data set from the levelling data is displayed to help with visualising the correlation between the two data sets. Another similar pattern is represented by the decreasing velocities in the area closer to the crest of the dam towards the bottom of the dam, as well as decreasing velocities when moving from the middle towards the extremities of the dam (toward both of the roads). Similar pattern is visible when comparing the levelling data with the second InSAR data set from 2015-2021 (Fig. 17), however the velocities are slightly reduced by 1-2 mm compared to the previous set.

All of these observations from three different methods appear to be showing similar overall trends throughout the dam's body on both the crest and the downstream side of it. It appears that the displacement is more intense in the upper part of the dam, starting with the crest, and decreasing in variety while moving down with the observations from both the InSAR and levelling methods. The other observation is given by the overall trend of the displacements from north to south, where on each berm there appears to be a middle which shows higher varieties throughout the whole berms, this being a similar trend which appears in the GPR data as well, showing a slight subsidence in the area of highest vertical negative displacement in the crest levelling data.

## 4. CONCLUSIONS

Three different methods have been assessed and an integration of the data has been attempted in order to provide information from different perspectives, for a better understanding of the vertical displacement behaviour of the embankment - rockfill with clay core dam, Poiana Mărului in Romania.

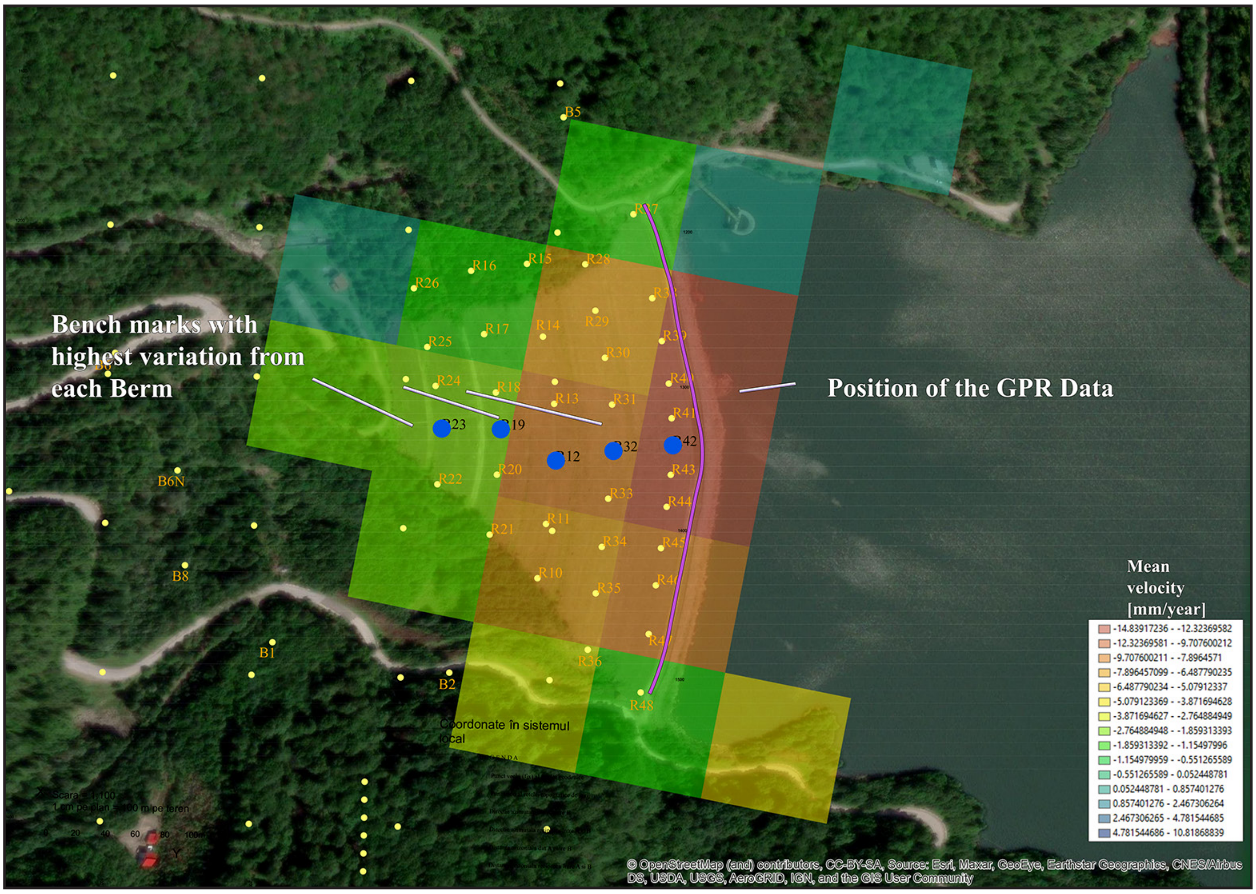

**Fig. 16.** Overlapping in GIS the InSAR data from 2018-2022 with the levelling benchmarks position, highlighting (blue dots) the benchmarks with highest variation from each berm.

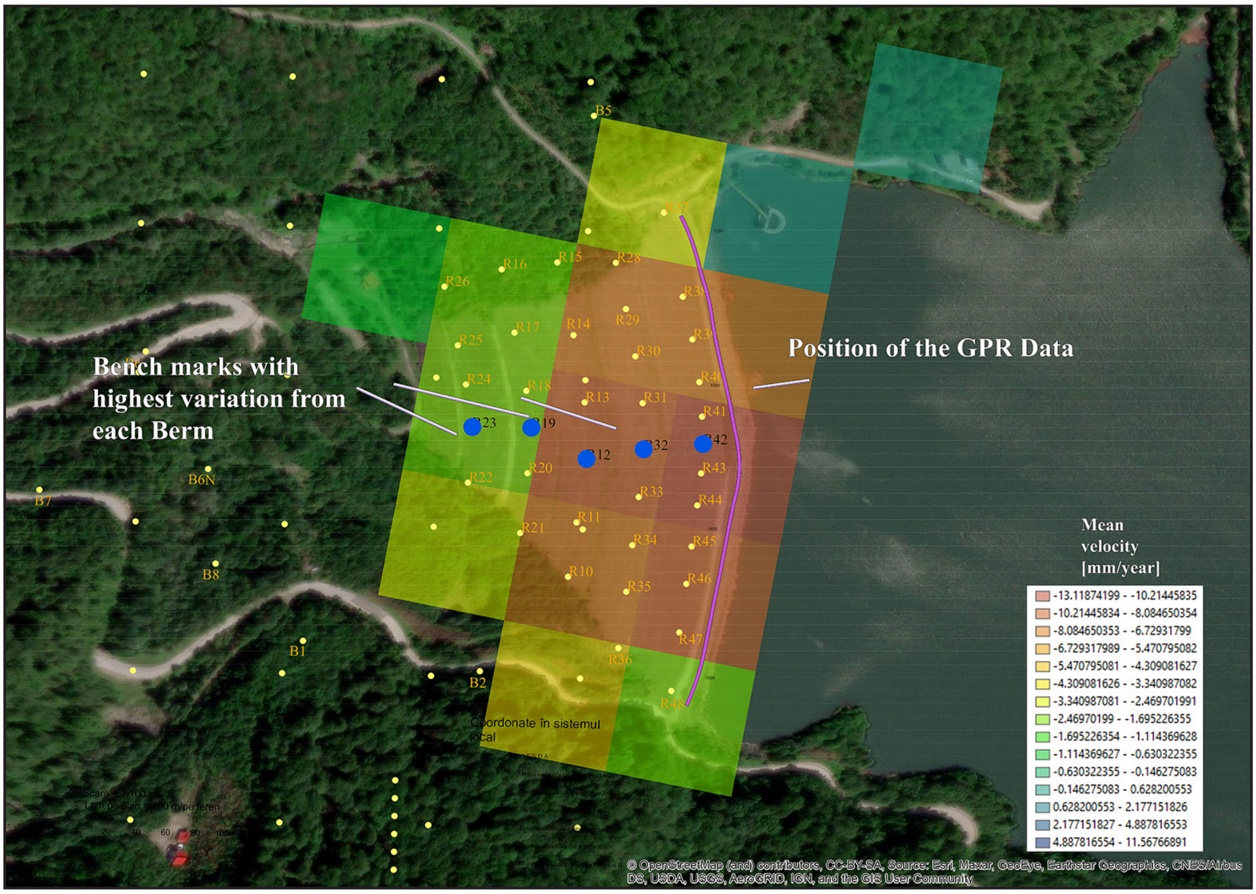

**Fig. 17.** Overlapping in GIS the InSAR data from 2015-2020 with the levelling benchmarks position, highlighting (blue dots) the benchmarks with highest variation from each berm.

The annual topo-geodetic surveys offer important information about the behaviour in time of the hydropower dams. In the case of the Poiana Mărului dam, the data shows a tendency in terms of negative displacements or subsidence appearing regularly in the area close to the upper- middle of the dam. Even though these movements are still in the normal displacement values to comply with the functionality standards regarded by the law, specific to these types of dams, and the levelling method provides high accuracy and precision of these type of measurements, the topo-geodetic data does not provide more information about the internal structure of the construction, where the GPR data comes in with new information.

The GPR method managed to show information from the body of the dam's core, down to approximately 4 m. The GPR data highlights different layers in the top part of the dam interpreted as foundation layers, which appear to have different thicknesses, and highlights an area of slight subsidence which appears to correlate with the levelling data. In general, the GPR data provides a subsurface imaging and characterisation of the top metres of the crest which can help in the future with better localised repair attempts for example. Even though the GPR method has limitations in terms of its applications in areas rich in clay content, it appears that on this dam it allowed for highlighting features of interest. And as the Poiana Mărului dam is made of rock and in theory only its core is made of clay, due to the positioning of the GPR profiles, data was collected mostly from the clay part of the dam.

The publicly available InSAR data from the European Ground Motion Service (EGMS), even though with a very low pixel resolution, still provides a significant amount of data coverage and precision in order to observe similar trends when compared to the annual levelling surveys. It appears that other dams in Romania are not as well covered with processed InSAR data points for vertical displacement analysis, where the position of the Poiana Mărului dam and the orientation, makes it a good candidate for these kinds of studies. InSAR methods have the advantage of reaching mm precision without the need of field surveys (or with minimal field surveys) and have the potential of offering real time displacement information as the satellites are orbiting the Earth every 6 days which comes with new data sets. For a better correlation of the individual values though, there is a need for a higher resolution, which can be achieved by processing individual data regularly, and incorporating a

DEM data set with a much higher resolution. However, the platform still proves to provide significant information about the overall displacement trend of the dam's body.

Correlating all of these data together was done in ArcGIS proved to be a very easy way to handle data from different types of methods, which allows for better overviews and overlaps of the data from different sets and to extract useful information from areas of interest.

The Poiana Mărului dam appears to have an overall trend and characteristics in terms of vertical displacement spread across the dam's body, and all of these methods fit in to provide a better overview of the dam's behaviour through time.

## ACKNOWLEDGEMENTS

The authors would like to extend their sincere appreciation to Prof. Dr. Eng. Cornel Păunescu and Cornel & Cornel Topoexim SRL for their invaluable assistance and support throughout this project, and to Roxana Stănescu for their supportive roles in the topo-geodetical part of the study. Our gratitude also goes to Gerea Gheorghe and Alexandru Micu for their essential logistical support and help in geophysical data collection. We are particularly thankful to Dr. Eng. Traian Moldoveanu, Mihai Duțu, and Mihaela Istrate for providing geophysical equipment. Additionally, our heartfelt thanks to Hidroelectrica S.A. for allowing access to the dam sites, and we are equally grateful to Bijan Nistor.

## REFERENCES

Adamo, N., Al-Ansari, N., Sissakian, V., Laue, J., Knutsson, S. (2021). Geophysical Methods and their Applications in Dam Safety Monitoring. *J. Geotech. Eng.*, **11** (*1*): 291-345.

Alonso-Díaz, A., Casado-Rabasco, J., Solla, M., Lagüela, S. (2023). Using InSAR and GPR Techniques to Detect Subsidence: Application to the Coastal Area of "A Xunqueira" (NW Spain). Remote Sens. **15**: 3729.

Avram, D., Preotescu, C., Caldarea, G., Bratosin, I., Kivu, R. (2017). Method of tracking deformations for hydrotechnic dams structures. *J. Geotech. Eng.*, **5**: 151-160.

Batrakov, D.O., Antyufeyeva, M.S., Antyufeyev, A.V., Batrakova, A.G. (2017). GPR data processing for evaluation of the subsurface cracks in road pavements. 2017 9th International Workshop on Advanced Ground Penetrating Radar (IWAGPR): 1-6, Edinburgh, UK.

Busetti, A., Calligaris, C., Forte, E., Areggi, G., Mocnik, A., Zini, L. (2020). Non-Invasive Methodological Approach to Detect and Characterize High-Risk Sinkholes in Urban Cover Evaporite Karst: Integrated Reflection Seismics, PS-InSAR, Leveling, 3D-GPR and Ancillary Data. A NE Italian Case Study. *Remote Sens.* **12:** 3814.

Capes, R., Passera, E. (2023). End-to-end implementation and operation of the European Ground Motion Service (EGMS) - Product Description and Format Specification, **2**.

Cetin, H., Laman, M., Ertunç, A. (2000). Settlement and slaking problems in the world's fourth largest rock-fill dam, the Ataturk Dam in Turkey. *Eng. Geol.*, **56**(*3-4*): 225-242.

Chun-Hun, L., Chih-Pin, L., Yin-Chun, H., Chih-Chung, C., Po-Lin, W., Hsin-Chan, L. (2018). Application of geophysical methods in a dam project: Life cycle perspective and Taiwan experience. *J. Appl. Geoph.*, **158**: 82-92.

Coșarcă, C. (2003). Topografie inginerească. Ed. Matrix Rom, București.

Daniels, D.J. (2004). Ground Penetrating Radar. 2nd Edition, IEE Radar, Sonar and Navigation Series, **15** (Ed.). The Institution of Electrical Engineers, London. http://dx.doi.org/10.1049/pbra015e

Conyers, L.B. (2004). Ground-Penetrating Radar for Archaeology. Alta Mira Press, Walnut Creek, 203 p.

De Giorgi, L., Leucci, G. (2014). Detection of Hazardous Cavities below a Road Using Combined Geophysical Methods. *Surv. Geophys.*, **35**: 1003-1021.

Gerea, A.G., Mihai, A.E. (2023). Case Studies and Lessons on Using the GPR Method on Hydropower Dams in Romania. 12th International Workshop on Advanced Ground Penetrating Radar (IWAGPR) 2023: 1-4, Lisbon, Portugal.

Hamran, S.E., Paige, D.A., Allwood, A., Amundsen, H.E.F., Berger, T., Brovoll, S., Carter, L., Casademont, T.M., Dypvik, H., Eide, S., Fairen, A.G., Ghent, R., Kohler, J., Mellon, M.T., Nunes, D.C., Plettemeier, D., Russell, P., Siegler, M., Øyan, M.J. (2022). Ground penetrating radar observations of subsurface structures in the floor of Jezero crater. *Mars. Sci,* Adv.8,eabp8564.

Kayode, O.T., Odukoya, A.M., Adagunodo, T.A., Adeniji, A.A. (2018). Monitoring of seepages around dams using geophysical methods: a brief review. *IOP Conf. Ser. Earth Environ. Sci.*, **173**: 012026.

Loperte, A., Bavusi, M., Cerverizzo, G., Lapenna, V., Soldovieri, F. (2011). Ground Penetrating Radar in Dam Monitoring: The Test Case of Acerenza (Southern Italy). *Int. J. Geoph.*, 9 p.

Marchamalo-Sacristán, M., Ruiz-Armenteros, A.M., Lamas-Fernández, F., González-Rodrigo, B., Martínez-Marín, R., Delgado-Blasco, J.M., Bakon, M., Lazecky, M., Perissin, D., Papco, J., Sousa, J.J. (2023). MT-InSAR and Dam Modeling for the Comprehensive Monitoring of an Earth-Fill Dam: The Case of the Benínar Dam (Almería, Spain). *Remote Sens.*, **15**: 2802.

Nistor, G. (1998). Teoria prelucrării măsurătorilor geodezice. Rotaprint Publishing House, Iași.

Nistor, G. (1993). Geodezia aplicată la studiul construcțiilor. Editura Gheorghe Asachi, Iași.

Ohmachi, T., Tahara, T. (2011). Nonlinear Earthquake Response Characteristics of a Central Clay Core Rockfill Dam. *Soils and Foundations*, **51**(*2*): 227-238.

Popovici, A. (2002). Baraje - pentru acumulări de apă, vol. 2, Editura Tehnică, România.

Prișcu, R. (1974). Construcții hidrotehnice, vol. I, Editura Didactică și Pedagogică, București.

Pueyo Anchuela, Ó., Frongia, P., Di Gregorio, F., Casas Sainz, A.M., Pocoví Juan, A. (2018). Internal characterization of embankment dams using ground penetrating radar (GPR) and thermographic analysis: A case study of the Medau Zirimilis Dam (Sardinia, Italy). *Eng. Geol.,* **237**: 129-139.

Reynolds, J. M. (2011). An Introduction to Applied and Environmental Geophysics. New York, NY, Wiley-Blackwell Publishing, 712 p.

Ruiz-Armenteros, A.M., Marchamalo-Sacrsitán, M., Bakoň, M., Lamas-Fernández, F., Delgado, J.M., Sánchez-Ballesteros, V., Papco, J., González-Rodrigo, B., Lazecky, M., Perissin, D., Sousa, J.J. (2021). Monitoring of an embankment dam in southern Spain based on Sentinel-1 Time-series InSAR. *Procedia Computer Science*, **181**: 353-359.

Sims, G.P. (1994). Aging of Masonry Dams. *Proc, Instit. Civ. Eng. - Water, Maritime and Energy*, **106**(*1*): 61-70.

Stănescu, R.A., Nache, F., Păunescu, C. (2017). Monitoring the vertical and horizontal displacements of the Poiana Mărului dam. *J. Geod., Cartog. Cad./UGR*.

Xu, X., Zeng, Q., Li, D., Wu, J., Wu, X., Shen, J. (2010). GPR detection of several common subsurface voids inside dikes and dams. *Eng. Geol.,* **111**(*1-4*): 31-42.

## Accessed internet links

Detektia. Available online: https://detektia.com/en/insar/ps-insar-ds-insar/ (accessed on 15.01.2024).

EGMS - European Ground Motion Service. Available online: https://egms.land.copernicus.eu/ (accessed on 25.01.2024).

Hidroconstructia. Available online: https://www.hidroconstructia.com/dyn/2pub/proiecte_det.php?id=38&pg=20 (accessed on 07.12.2023).

Hidroelectrica. Available online: https://www.hidroelectrica.ro/article/36 (accessed on 07.12.2023).

## Other references

Romanian Law nr. 466, 18 July 2001, on hydropower dam safety.